# Enhancement of the North Atlantic $CO_2$ sink by Arctic Waters

Jon Olafsson[1], Solveig R. Olafsdottir[2], Taro Takahashi[3,5], Magnus Danielsen[2] and Thorarinn S. Arnarson[4,5]

[1] Institute of Earth Sciences, Sturlugata 7 Askja, University of Iceland, IS 101 Reykjavik, Iceland. jo@hi.is
[2] Marine and Freshwater Research Institute, Fornubúðir 5, IS 220 Hafnafjörður, Iceland
[3] Lamont-Doherty Earth Observatory of Columbia University, Palisades, NY 10964, U.S.A.
[4] National Energy Authority, Grensásvegur 9, IS 108 Reykjavík, Iceland
[5] Deceased

## Abstract

The North Atlantic north of 50°N is one of the most intense ocean sink areas for atmospheric $CO_2$ considering the flux per unit area, 0.27 Pg-C $yr^{-1}$, equivalent to -2.5 mol C $m^{-2}$ $yr^{-1}$. The Northwest Atlantic Ocean is a region with high anthropogenic carbon inventories. This is on account of processes which sustain $CO_2$ air-sea fluxes, in particular strong seasonal winds, ocean heat loss, deep convective mixing and $CO_2$ drawdown by primary production. The region is in the northern limb of the Global Thermohaline Circulation, a path for the long term deep sea sequestration of carbon dioxide. The surface water masses in the North Atlantic are of contrasting origins and character, on the one hand the northward flowing North Atlantic Drift, a Gulf Stream offspring, on the other hand southward moving cold low salinity Polar and Arctic Waters with signatures from Arctic freshwater sources. We have studied by observations, the $CO_2$ air-sea flux of the relevant water masses in the vicinity of Iceland in all seasons and in different years. Here we show that the highest ocean $CO_2$ influx is to the Arctic and Polar waters, respectively, -3.8±0.4 mol C $m^{-2}$ $yr^{-1}$ and -4.4±0.3 mol C $m^{-2}$ $yr^{-1}$. These waters are $CO_2$ undersaturated in all seasons. The Atlantic Water is a weak or neutral sink, near $CO_2$ saturation, after poleward drift from subtropical latitudes. These characteristics of the three water masses are confirmed by data from observations covering 30 years. We relate the Polar and Arctic Water persistent undersaturation and $CO_2$ influx to the excess alkalinity derived from Arctic sources. Carbonate chemistry equilibrium calculations indicate clearly that the excess alkalinity may support at least 0.058 Pg-C $yr^{-1}$, a significant portion of the North Atlantic $CO_2$ sink. The Arctic contribution to the North Atlantic $CO_2$ sink which we reveal is previously unrecognized. However, we point out that there are gaps and conflicts in the knowledge about the Arctic alkalinity and carbonate budgets and that future trends in the North Atlantic $CO_2$ sink are connected to developments in the rapidly warming and changing

Arctic. The results we present need to be taken into consideration for the question: Will the North Atlantic continue to absorb $CO_2$ in the future as it has in the past?

## 1 Introduction

The oceans take up about a quarter of the annual anthropogenic $CO_2$ emissions (Friedlingstein et al., 2019). This may even be an underestimate (Watson et al., 2020). The North Atlantic north of 50°N is one of the most intense ocean sink areas for atmospheric $CO_2$ considering the flux per unit area (Takahashi et al., 2009). The reasons are strong winds and large natural partial pressure differences, $\Delta pCO_2=(pCO_{2sw} - pCO_{2a})$, between the atmosphere and the surface ocean. The $\Delta pCO_2$ in seawater is a measure of the escaping tendency of $CO_2$ from seawater to the overlying air. The $\Delta pCO_2$ is proportional to the concentration of undissociated $CO_2$ molecules, $[CO_2]aq$, which constitutes about 1 % of the total $CO_2$ dissolved in seawater (the remainders being about 90-95 % as $[HCO_3^-]$ and 4-9 % as $[CO_3^{2-}]$). The seawater $pCO_2$ depends sensitively on temperature and the $TCO_2$/Alk ratio, the relative concentrations of total $CO_2$ species dissolved in seawater ($TCO_2 = [CO_2]aq + [HCO_3^-] + [CO_3^{2-}]$) and the alkalinity, Alk, which reflects the ionic balance in seawater. Large $\Delta pCO_2$ has been attributed to, a) a cooling effect on the $CO_2$ solubility in the poleward flowing Atlantic Water, b) an efficient biological drawdown of $pCO_2$ in nutrient rich subpolar waters and c) high wind speeds over these low $pCO_2$ waters (Takahashi et al., 2002). Evaluations of $\Delta pCO_2$ based on observation and models have indicated that the Atlantic north of 50°N and northward into the Arctic takes up as much as 0.27 Pg-C $yr^{-1}$, equivalent to -2.5 mol C $m^{-2}$ $yr^{-1}$ (Takahashi et al., 2009;Schuster et al., 2013;Landschützer et al., 2013;Mikaloff Fletcher et al., 2006). The North Atlantic is a relatively well observed region of the ocean (Takahashi et al., 2009;Bakker et al., 2016;Reverdin et al., 2018). Nevertheless, estimates of long term trends for the North Atlantic $CO_2$ sink due to changes in either $\Delta pCO_2$ or wind strength are conflicting, particularly the Atlantic Water dominated regions (Schuster et al., 2013;Landschützer et al., 2013;Wanninkhof et al., 2013). The drivers of seasonal flux variations are considered inadequately understood (Schuster et al., 2013) and a mechanistic understanding of high latitude $CO_2$ sinks is regarded incomplete (McKinley et al., 2017). It has been common to many large scale flux evaluations, modelled or from observations, that they are based on regions defined by geographical borders, latitude and longitude, e.g. between 49°N and 76°N for the high latitude Sub Polar North Atlantic (Takahashi et al., 2009;Schuster et al., 2013). A more realistic approach is to define biogeographical regions,

biomes (Fay and McKinley, 2014). The influence of oceanographic property differences within this region on $CO_2$ fluxes has generally not been apparent, primarily due to Arctic latitude data limitations. The ability of current generation Earth System Models to predict trends in North Atlantic $CO_2$ has recently been questioned and suggested that their inadequacies may be caused by biased alkalinity in the simulated background biogeochemical state (Lebehot et al., 2019).

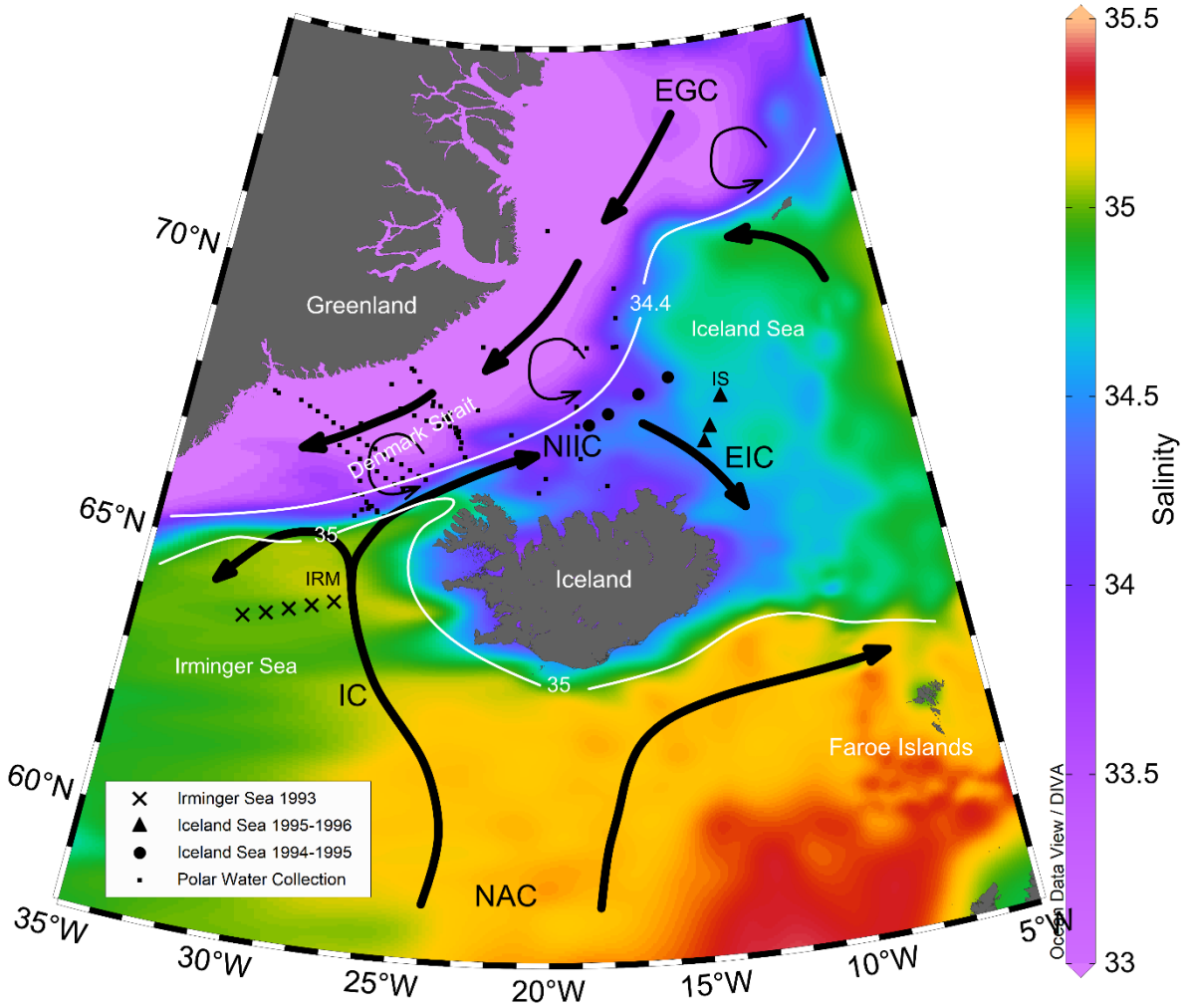


***Figure 1. Mean July to September surface salinity in the vicinity of Iceland.*** *The S=35 isohaline marks the bounday between northward flowing Atlantic Water and southward flowing cold Arctic Water and low salinity Polar Water. Stations in Irminger Sea marked X and stations in Iceland Sea marked ●for 1994-1995 and ▲for 1995-1996 observations. Collection of Polar Water stations 1983-2012 marked ▪. IRM and IS mark the location of time series stations. NAC: North Atlantic Current, IC: Irminger Current, NIIC: North Iceland Irminger Current, EIC: East Icelandic Current, EGC: East Greenland Current. Map based*

*on the NISE dataset (Nilsen et al., 2008) and drawn using the Ocean Data View program (Schlitzer, 2018).*

The high latitude North Atlantic Ocean in the vicinity of Iceland, is a region of contrasting surface properties (Fig. 1). The northward flowing North Atlantic Current carries relatively warm and saline Atlantic Water, derived from the Gulf Stream, as far as the Nordic Seas and the Arctic Ocean north of Svalbard. The Irminger Current branch carries Atlantic Water to south and west Iceland and a small branch, the North Icelandic Irminger Current that transports 1 Sv (1 Sv=$10^6$ $m^3$ $s^{-1}$), reaches the Iceland Sea (Stefánsson, 1962;Våge et al., 2011). The temperature and salinity properties of the Atlantic Water are known to change with atmospheric forcing and with freshening events (Dickson et al., 1988;Hátún et al., 2005;Holliday et al., 2020). The rapid East Greenland Current (EGC) (Håvik et al., 2017) flows southward from the Arctic to the North Atlantic, carrying Polar Water cold and with low salinity, S<34.4, due to ice melt and a portion of the large freshwater input to the Arctic from rivers that contribute about 11% of the global riverine discharge (Sutherland et al., 2009;McClelland et al., 2012). In between these extremes there are large areas of the Greenland and Iceland Seas that contain predominantly the intermediate, Arctic Water which is a product of heat loss and freshwater export from the EGC (Fig. 1) (Våge et al., 2015). The north- and southward flowing currents are separated by the Arctic Front outlined in Figure 1 by the salinity=35 contour generally oriented SW-NE. Deep water formation in the high latitude North Atlantic produces cold dense waters which, together with a similar product in the Labrador Sea, are source waters for the Global Thermohaline Circulation linking the regional air-sea $CO_2$ flux to a route for the long term deep ocean sequestration of anthropogenic $CO_2$ (Broecker, 1991). Downstream from the Polar Water and Arctic Water southward flows is the subpolar North Atlantic with high water column inventories of anthropogenic carbon (Khatiwala et al., 2013;Gruber et al., 2019). The high anthropogenic $CO_2$ regions have been attributed to the combined effects of the solubility and biology gas exchange pumps on the $CO_2$ fluxes (Takahashi et al., 2002). The region of our study affects large scale ocean-atmosphere $CO_2$ exchange processes in the North Atlantic.
Here we evaluate regional, seasonal and interannual air-sea carbon dioxide fluxes for the main surface waters characteristic of this region (Fig. 1). We base this work on extensive observations which cover regional water masses, all seasons and include different states of the North Atlantic Ocillation, NAO (Flatau et al., 2003). We employ two different observation approaches for flux estimates. Firstly, repeat station hydrography with emphasis on the

seasonal flux patterns in Atlantic Water and in Arctic Water (Fig. 1). Secondly, underway ship records of surface $pCO_2$ where the emphasis was on the different surface water masses (Fig. 2).

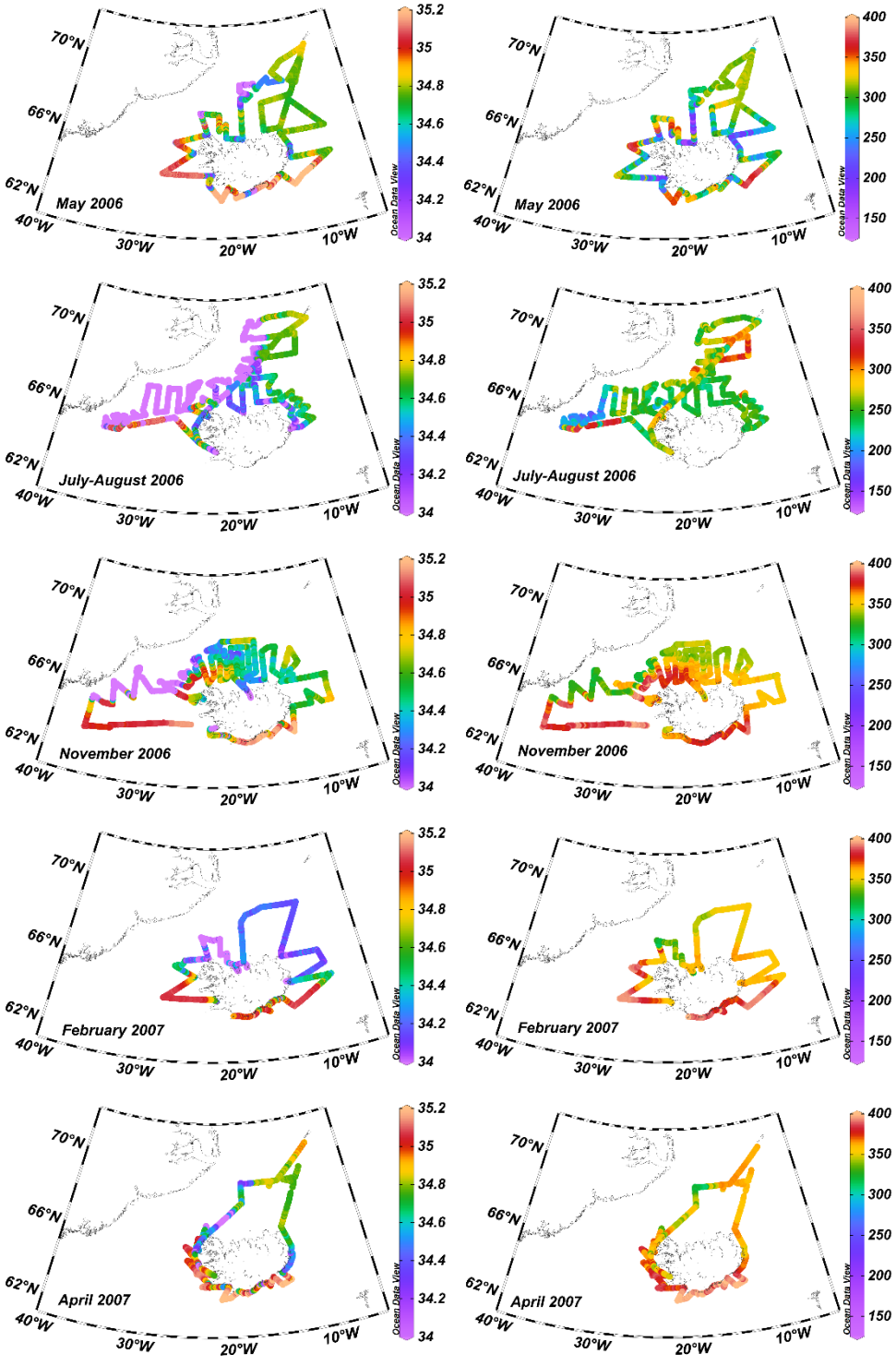

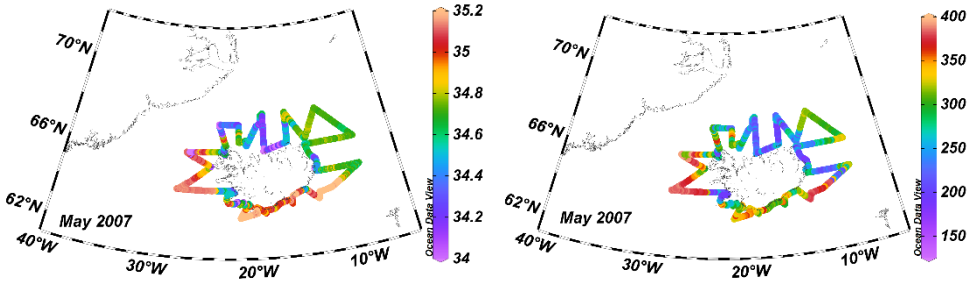


**Figure 2. Cruise tracks where surface layer salinity and $pCO_2$ were recorded underway.** Left sea surface salinity, right $pCO_2$sw(µatm) along the cruise tracks. Maps drawn using the Ocean Data View program (Schlitzer, 2018).

We describe long term carbon chemistry characteristics of water masses in mid winter when physical forces prevail over biological processes. For the Irminger Sea and Iceland Sea from time series observations (Olafsson et al., 2010) and for the EGC Polar Water from a collection of $pCO_2$ data assembled in the period 1983 to 2012.

## 2 Methods

### 2.1 Data acquisition

#### 2.1.1 Seasonal studies 1993-1996

Seasonal carbon chemistry variations in the relatively warm and saline (S>35) Atlantic Water were studied 1993-1994 on 15 cruises from February 1993 to January 1994 with 5 stations on a 167 km long transect over the core of the Irminger Current and into the northern Irminger Sea (Fig. 1 and Tables S1 and S2). In order to close the full annual cycle, to 23 February 1994 we use data from the previous year and date. In 1994-1996 the study centered on the colder and less saline Arctic Water of the Iceland Sea and was conducted on 22 cruises with sampling dates from 11 Feb 1994 to 12 Feb 1996

. In 1994 on 4 stations on a 168 km long transect into the Iceland Sea Gyre and in 1995 on 3 stations across the East Icelandic Current (Fig. 1 and Tables S1 and S3 in the supplement). On each cruise the station work was completed in 1-2 days. For both regions, the timing of cruises was with the period of the phytoplankton spring bloom in mind (Takahashi et al., 1993). The work was conducted on vessels operated by the Marine Research Institute (MRI) in Reykjavik, Iceland, R/V Bjarni Seamundsson and R/V Arni Fridriksson. Three times in

1994 a fishing vessel M/V Solrun, was hired. In August 1994 the stations were completed on the Norwegian vessel R/V Johann Hjort.

Discrete surface layer, 1m, 5m and 10m, $pCO_2$ samples were collected into 500 ml volumetric flasks and total dissolved inorganic carbon samples, TCO2, into 250 ml flasks from water bottles on a Rosette and Sea Bird 911 CTD instruments. The $pCO_2$ samples were preserved with mercuric chloride and analysed ashore by equilibration at 4°C with a gas of known $CO_2$ concentration followed by gas chromatography with a flame ionization detector. The instrument was calibrated with $N_2$ reference gas and 3 standards, 197.85 ppm, 362.6 ppm and 811.08 ppm, calibrated against standards certified by NOAA-CMDL at Boulder, CO, USA. The standards used for the underway measurements were similarly calibrated (Chipman et al., 1993). Samples for total dissolved inorganic carbon, TCO2, were similarly preserved with mercuric chloride and analysed by coulometry ashore. Quality assurance and sample storage experiments indicated an overall precision of the discrete sample $pCO_2$ determinations better than ±2 µatm and of the TCO2 determinations ±2 µmol $kg^{-1}$ after1990 but ±4 µmol $kg^{-1}$ earlier (Olafsson et al., 2010).

### 2.1.2 Underway $pCO_2$ records 2006-2007

The underway $pCO_2$ determinations in 2006-2007 covered areas of the East Greenland Current in and northwards from the Denmark Strait, in addition to Atlantic and Arctic Waters. The 6 cruises (Table S4) covered all seasons and all three water masses but with variable areal extensions (Fig. 2). Seawater was pumped continuously from an intake at 5 m depth at 10 L $min^{-1}$ into a shower-head equilibrator with a total volume of 30 L and a headspace of 15 L. Temperature at the inlet and salinity were measured with an SeaBird Model SBE-21 thermosalinograph (Sea-Bird Electronics, Seattle,WA, USA). Underway $pCO_2$ determinations were carried out with a system similar to the one described by Bates and coworkers (Bates et al., 1998). The mole fraction of $CO_2$ (V $CO_2$) in the headspace was determined with a Li-Cor infrared analyzer Model 6251 (Li-Cor Biosciences, Lincoln, NB, USA). The instrument was calibrated against four standards of $CO_2$ in air certified by NOAA-CMDL at Boulder, CO, USA. and a $N_2$ reference gas. The standards had $CO_2$ dry air mole fractions of 122.19, 253.76, 358.41 and 476.81 ppm. The $pCO_2$ sw determinations were corrected to in-situ seawater temperatures using the equation (Takahashi et al., 1993):

$$pCO_2 \text{ sw(in situ)} = pCO_2 \text{ sw(eq)} \; e^{0.0423(T_{in\ situ} - T_{eq})} \qquad \text{(eq.1)}$$

The precision of the underway $pCO_2$ determinations is estimated by SOCAT better than ±5 µatm (Bakker et al., 2016).

### 2.1.3 Time series data

We use discrete sample $pCO_2$ andTCO2 data to calculate Total Alkalinity from the Irminger Sea and the Iceland Sea time series stations (Ólafsson, 2012, 2016).

### 2.1.4 Polar Water data collection

Discrete samples for carbon chemistry studies were taken on stations (N=146) in the East Greenland Current when opportunites permitted on cruises in the period 1983 to 2012. The 25 m surface layer data include >400 TCO2 samples and >300 pairs of $pCO_2$ and TCO2 for calculation of carbonate system parameters. The sesonal cycle by month is evaluated from the composite data.

### 2.1.5 Carbonate chemistry calculations

The most desireable way for computing carbonate chemistry parameters is to use $pCO_2$ and TCO2 (Takahashi et al., 2014). We calculate Total alkalinity from discrete sample $pCO_2$ and TCO2 data pairs using the CO2SYS.xls v2.1 software (Lewis and Wallace, 1998;Pierrot et al., 2006) and select carbonic acid dissociation constants (Lueker et al., 2000), the constant for $HSO_4$- (Dickson, 1990) and boron concentrations (Lee et al., 2010).

## 2.2 $CO_2$ air-sea flux calculations

In this study, the partial pressure of carbon dioxide in seawater samples has been measured by gas-seawater equilibration methods (Olafsson et al., 2010). The results are expressed as $pCO_2$. The bulk flux of the carbon dioxide across the air-sea interface is often estimated from its relationship with wind speed and sea-air partial pressure difference, $\Delta pCO_2$. We determine the flux (F) from $\Delta pCO_2$ and use Eq. 2 and Eq. 3 for estimating the bulk air-sea fluxes of $CO_2$ (Takahashi et al., 2009)

$$F = k \cdot \alpha \cdot \Delta pCO_2 \qquad \text{(Eq 2)}$$

$$F = 0.251\ U^2\ (Sc/660)^{-0.5}\ \alpha\ (pCO_{2\ w} - pCO_{2\ a}) \qquad \text{(Eq 3)}$$

There $k=0.251\ U^2\ (Sc/660)^{-0.5}$ is the gas transfer velocity or kinetic component of the expression (Wanninkhof, 2014), $\alpha$ is the solubility of $CO_2$ gas in sea water (Weiss, 1974) and $\Delta pCO_2 = (pCO_{2sw} - pCO_{2a})$, is the partial pressure difference or thermodynamic component of the expression (Takahashi et al., 2009). For the wind speed, U, we use the CCMP-2

reanalysis wind product (Wanninkhof, 2014;Atlas et al., 2011;Wanninkhof and Triñanes, 2017).

The atmospheric partial pressure values, $pCO_{2\ a}$, used in the $\Delta pCO_2$ calculations are weekly averages from the GLOBALVIEW-CO2 database for the CO2-ICE location which is at Vestmannaeyjar islands, off south Iceland (GLOBALVIEW-CO2, 2013). Mauna Loa values were used for periods where CO2-ICE data was missing, 1983-1992 and 2010-2012 (Tans and Keeling, 2019). The dry air V $CO_2$ mole fraction values were converted to µatm using $pCO_2$ (µatm)= V $CO_2$ ($P_a - P_w$) where Pa is the barometric pressure and $P_w$ is the equilibrium water vapour pressure (Weiss and Price, 1980).

For the Irminger Sea seasonal study we use 30 day running means of the squared daily wind speed for the region 63.5°N to 64.5°N and 27°W to 32°W and for the Iceland Sea seasonal study a similar wind product for the region 66.5°N to 68.5°N and 12°W to 19°W. Fluxes were calculated for the periods between cruises from interpolated $pCO_2$ data and period mean 30 day squared wind running means data. There are thus 14 flux periods covering a year for the Irminger sea and 21 flux periods covering two years in the Iceland Sea (Tables S1 and S2 in the supplement). The annual fluxes were found by summation of the period fluxes (Table 1).

For the underway cruises 2006 to 2007 we used CCMP-2 daily wind fields at 1x1 degree for the region 62°N to 72°N and 5°W to 40°W. This region was further divided into 4 sub-regions by latitude 64.9°N and longitude 20°W. Daily 30 day running means of the squared wind speed from two locations in each sub-region were extracted and their means used for flux calculations when the vessel sailed in the area. Fluxes were calculated for all $pCO_2$ data from the 6 cruises, in total 42938 measurements.

The flux data from each of the 6 cruises were categorized into the three sea water types using the following criteria:

1) Atlantic Water S>35, Arctic Water S: 34.4-34.9, Polar Water S<34.4.
2) Seasonal salinity and temperature variations were taken into account.
3) Waters with runoff influences from Iceland were excluded using salinity and ship position data.

Thus a total of 33352 measurements were used, or 78% of the flux data points. The $CO_2$ fluxes in the realm of each water mass were assessed for the duration of each cruise by numerical integration. Fluxes in the 5 periods between cruises were assessed by interpolation of temperature, salinity and $pCO_2$ for each water mass and by using period regional 30 day

running means of squared wind speed data. The annual flux for each water mass was assessed by summation.

## 3 Results

### 3.1 Seasonal variations and annual $CO_2$ fluxes at regional water masses

The wind gas transfer coefficient reveals seasonal variations reflecting strong winds in winter when they may be stronger over the Irminger Sea than the Iceland Sea as in 1993-1994 and in 1994-1995 (Fig. 3a, Fig. S1). Both the Irminger Sea and the Iceland Sea seasonal studies reveal the stongest $CO_2$ undersaturation, with negative $\Delta pCO_2$ of about 100 µatm in May at the time of the phytoplankton spring bloom (Fig. 3b). The undersaturation diminishes through the summer and autumn followed by a gradual return to winter conditions (Takahashi et al., 1985;Peng et al., 1987;Takahashi et al., 1993).

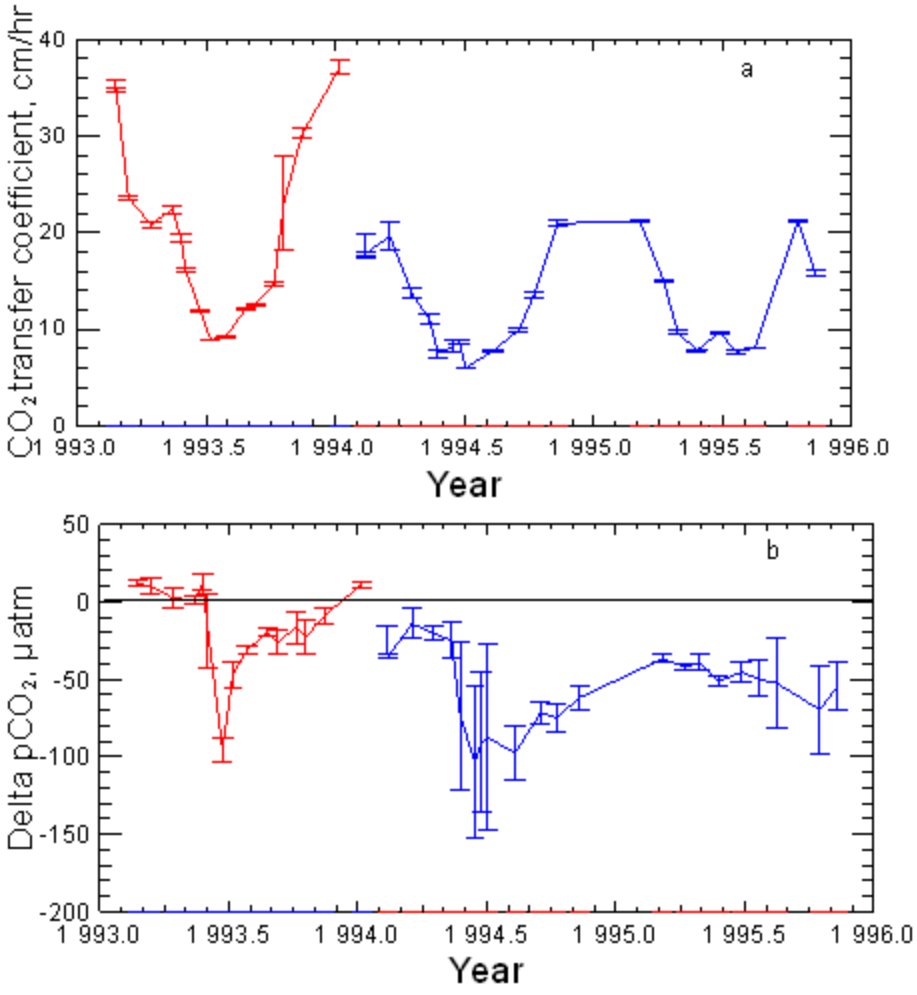

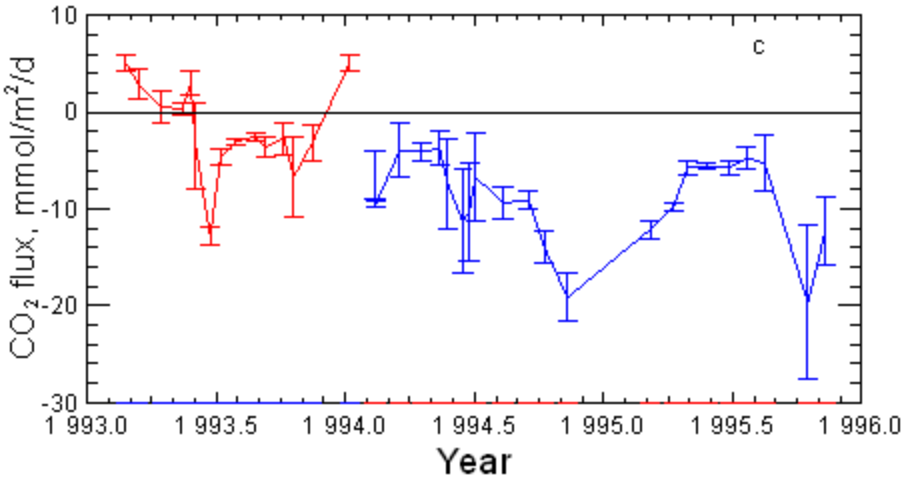


***Figure 3. Seasonal variations in the Atlantic Water of the Irminger Sea (red) and in the Arctic Water of the Iceland Sea (blue).*** *The gas transfer velocity (a) reflects the seasonal wind strength and the error bars its variations during intervals between cruises. Delta $pCO_2$ (b) records the tendency for $CO_2$ to be transferred to the atmosphere (positive) or from the atmosphere to the ocean (negative). The $CO_2$ flux rate (c) reveals that the Arctic Water is a $CO_2$ sink in all seasons whereas the Atlantic Water is a source in winter and a weak sink at other times of the year. The error bars indicate ± 1 standard deviation from the mean and reflect the variations between the stations observed each cruise.*

The $CO_2$ influx in the spring is, however, relatively small as the wind gas transfer coefficient is then moderate (Fig. 3a). In the autumn the winds strengthen with heat loss and vertical mixing while $CO_2$ undersaturation still persists. In mid winter, February-March, vertical mixing brings richer $CO_2$ water to the surface of the Irminger Sea leading to supersaturation (Ólafsson, 2003), the flux reverses and the region becomes a weak source for atmospheric $CO_2$ (Fig. 3c).

**Table 1 Annual sea–air $CO_2$ fluxes (mol C $m^{-2}$ $y^{-1}$) in the three water masses.**

| **Water masses and evaluation methods** | **$CO_2$ flux mol C $m^{-2}$ $y^{-1}$** |
|---|---|
| Atlantic water, repeat stations 1993 | -0.69±0.16 |
| Atlantic water, Underway Measurements, 2006-2007 | 0.07 ± 0.15 |
| Arctic water, repeat stations 1994 | -3.97±0.48 |
| Arctic water, repeat stations 1995 | -3.60±0.31 |
| Arctic water, Underway Measurements, 2006-2007 | -2.84 ± 0.19 |
| Polar water, Underway Measurements, 2006-2007 | -4.44 ± 0.34 |

The integrated annual $CO_2$ flux shows that the Atlantic Water in the Irminger Sea was a weak sink, -0.69±0.16 mol C $m^{-2}$ $y^{-1}$, in 1993 (Table 1). The more extensive underway area coverage of the Atlantic Water in 2006-2007, confirmed in essence the seasonal pattern and indicated that the Atlantic Water was a neutral sink, 0.07 ± 0.15 mol C $m^{-2}$ $y^{-1}$ for this year (Table 1). The winter gas transfer coefficient was again significantly larger over the Atlantic Water regions than the Arctic and Polar Waters, facilitating air-sea equilibration (Fig. 4b). The years of the Iceland Sea observations, 1994-1996, coincided with a large transition in the North Atlantic Ocillation (NAO) from a positive state 1994/1995 to a negative state in 1995/1996 and large scale shifts in ocean fronts (Flatau et al., 2003). Vertical density distribution in the Iceland Sea indicated an enhanced convective activity in 1995 (Våge et al., 2015). Cold northeasterly winds were persistent in the spring of 1995 resulting in record low temperature anomalies for the north Iceland shelf (Ólafsson, 1999). In 1995 the spring bloom associated undersaturation, $\Delta pCO_2$, was only half of that in 1994, possibly due to a weaker stratification in May and continued over the summer season (Fig.S2) (Våge et al., 2015). As in the Irminger Sea the spring bloom associated $CO_2$ influx is small. The largest $CO_2$ influx was in the fall and early winters of 1995 and 1996 as temperature dropped, winds gathered strength and vertical mixing was enhanced. This compensated for the small spring bloom in 1995 and the annual bulk fluxes 1994 and 1995 are similar and high despite very different physical conditions (Table 1). The UW$pCO_2$ surveys had less temporal resolution but confirmed all year undersaturation of the Arctic Water. However, the integrated annual influx, -2.84 mol C $m^{-2}$ $y^{-1}$, was significantly less than evaluated with repeat station data even though the strength of the gas transfer coefficient was similar in both studies (Table 1, Figs.4a and 4b). This may reflect the large underway area coverage compared with the repeated fixed stations.

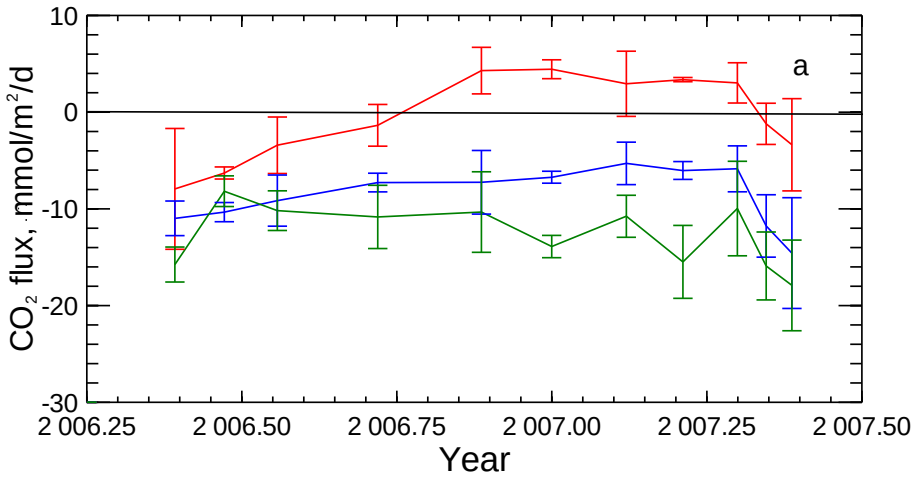

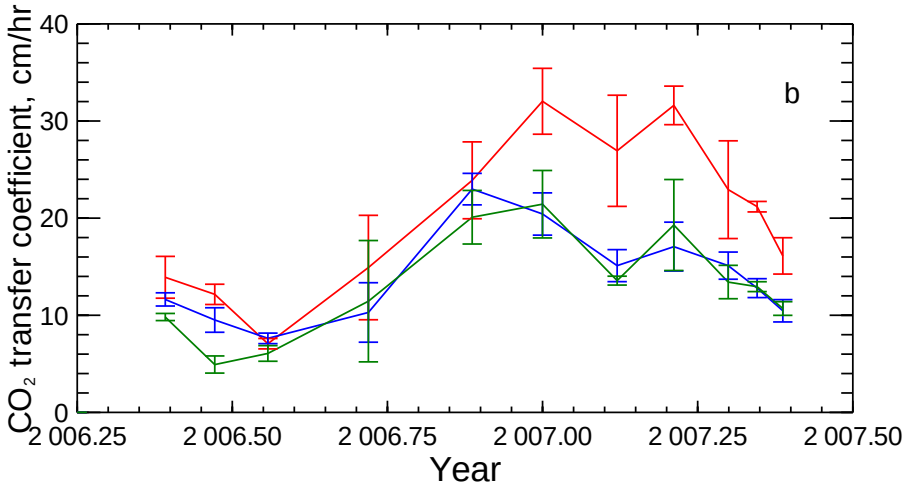


***Figure 4. Seasonal air-sea $CO_2$ flux variations from UW$pCO_2$ observations***. *a)Atlantic Water (red) is a weak sink in summer and neutral over the year, n=7068. Both Arctic Water (blue) n=16874, and Polar Water (green) n=9410, are strong sinks throughout the year. The error bars indicate ± 1 standard deviation from the mean. b) The gas transfer coefficient for the Atlantic Water regime is significantly stronger in winter than for the Arctic and Polar Water.*

Ice cover in the East Greenland Current is variable and the ice edge at the seasonal minimum has moved northward and from the Denmark Strait with decreasing Arctic sea ice (Serreze and Meier, 2019). The Polar Water salinity ranges from 34.4 to less than 30 in summer. The lowest salinity water freezes leading to salinity around 34 in winter. We covered the Polar Water in all six UW$pCO_2$ surveys 2006-2007 (Fig. 2) and undersaturation characterised this water mass in all cruises. The integrated annual influx, -4.44 mol C $m^{-2}$ $y^{-1}$ (Table 1, Fig.4), shows the Polar Water to be the strongest $CO_2$ sink, 80 % above the estimated mean for the Atlantic north of 50°N, -2.5 mol C $m^{-2}$ $y^{-}$(Takahashi et al., 2009). Further comparison with the Takahashi climatology indicates a broad agreement with Arctic Water region NE of Iceland with -3.5 to -4.5 mol C $m^{-2}$ $y^{-1}$ and with the Atlantic Water region S and SW of Iceland with about -1 mol C $m^{-2}$ $y^{-1}$ (Takahashi et al., 2009).

### 3.2 Long term Δ$pCO_2$ characteristics of the regional water masses

We evaluate the long term $pCO_2$ characteristics of the three water masses from three other data assembled over about 30 years. We use the Polar Water data collection and draft a composite picture of seasonal Δ$pCO_2$ variations in Polar Water in and north of the Denmark Strait (Fig.1) which confirms all year undersaturation, deep in summer, and in mid winter when salinity raises to ~ 34, the Δ$pCO_2$ levels at about -50 µatm (Fig. 5a). Long term winter Δ$pCO_2$ in the Irminger Sea and Iceland Sea (Figs. 1 and 5b) when biological activity is minimal (Olafsson et al., 2009), show the Atlantic Water to be slightly supersaturated and

following the atmospheric $pCO_2$ increase of 1.80 µatm/yr, whereas the Arctic Water is undersaturated to about -35 µatm. The Gulf Stream derived Atlantic Water which reaches the northern Irminger Sea and the Nordic Seas, has had a long contact time with the atmosphere to loose heat and reach near $CO_2$ saturation (Takahashi et al., 2002;Olsen et al., 2006).

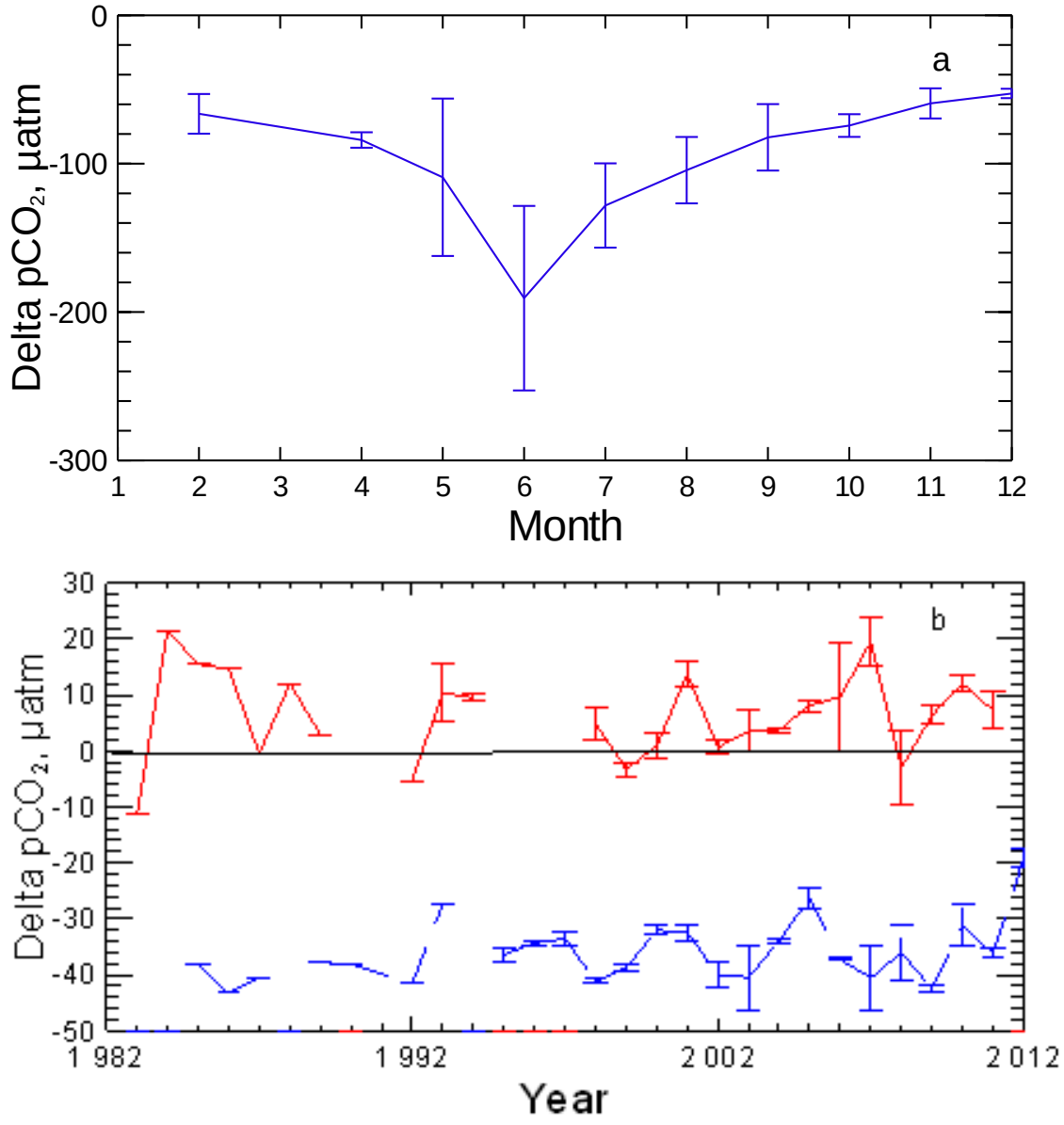


***Figure 5. Water mass decadal surface water $pCO_2$ characteristics.*** *a) A composite picture of Delta $pCO_2$ from 146 stations with Polar Water $pCO_2$ observations (n=312) from the 25 m surface layer 1983 to 2012 shows undersaturation at all times of the year. The error bars indicate ± 1 standard deviation from the monthly means. b) Atlantic Water at the Irminger Sea time series station (red) is generally a weak $CO_2$ source in winter (24 winters, 52 samples), January-March, whereas winter (25 winters, 61 samples) $CO_2$ undersaturation persits at the Iceland Sea time series site (blue). The error bars indicate ± 1 standard deviation from the surface layer station means.*

The Polar Water in the East Greenland Current which is advected southward from the Arctic is in general characterised by low temperature and large seasonal salinity and carbonate chemistry variations. Both physical and biogeochemical processes generate the large seasonal variability but the winter observations represent the state of lowest biological activity (Fig. 6) (Table 2). The TCO2 data in Table 2 are uncorrected for hydrographic variations or anthropogenic trends but the Atlantic Water is based on a short period of 10 years and the Polar Water atmospheric contact history is poorly known.

**Table 2. Mean IRM-TS Atlantic Water surface layer conditions in winter, 2001-2010 and in Polar Water 25 m surface layer November to April 1984-2012.**

| | T °C | Salinity, S | Density, ρ kg $m^{-3}$ | TCO2/S µmol $kg^{-1}$ $psu^{-1}$ | ALK/S µmol $kg^{-1}$ $psu^{-1}$ | TCO2/ALK | $pCO_2$ µatm |
|---|---|---|---|---|---|---|---|
| Atlantic Water | 7.11 ± 0.36 | 35.13 ± 0.03 | 1027.507 ± 0.034 | 61.11 ± 0.09 | 65.96 ± 0.13 | 0.926 ± 0.002 | 388 ±9 |
| Polar Water | -0.31 ±1.53 | 33.95 ± 0.33 | 1027.255 ± 0.244 | 62.16 ±0.54 | 66.49 ± 0.40 | 0.935 ± 0.004 | 301 ±11 |

The winter conditions in the northward flowing Atlantic Water at the Irminger Sea time series station 2001-2010 (Table 2) are in stark contrast and with notably higher $pCO_2$ and lower TCO2/S and ALK/ S ratios than the Polar Water in winter.

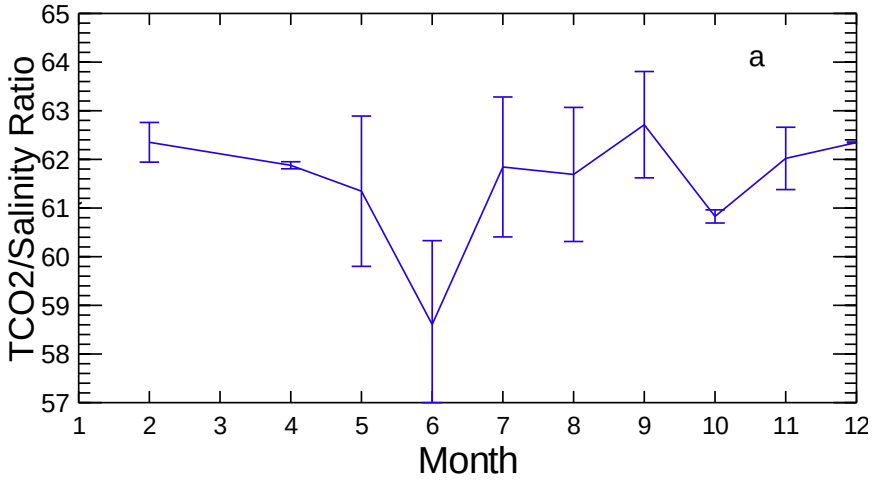

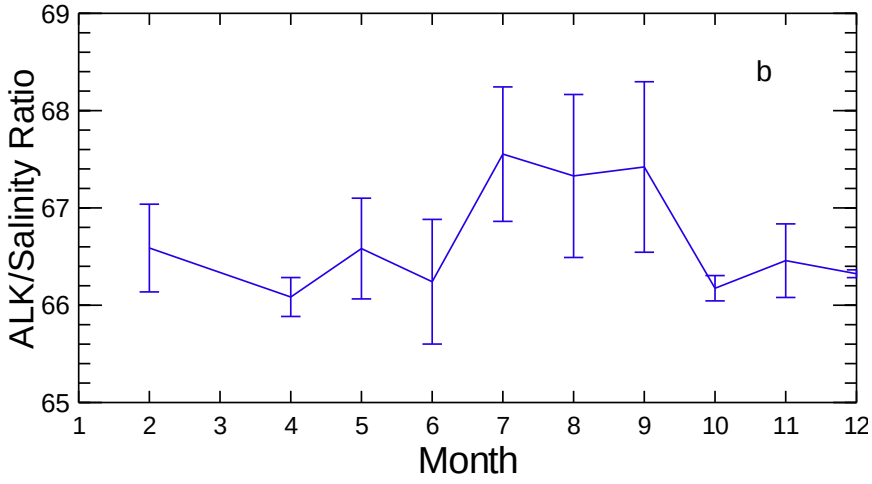


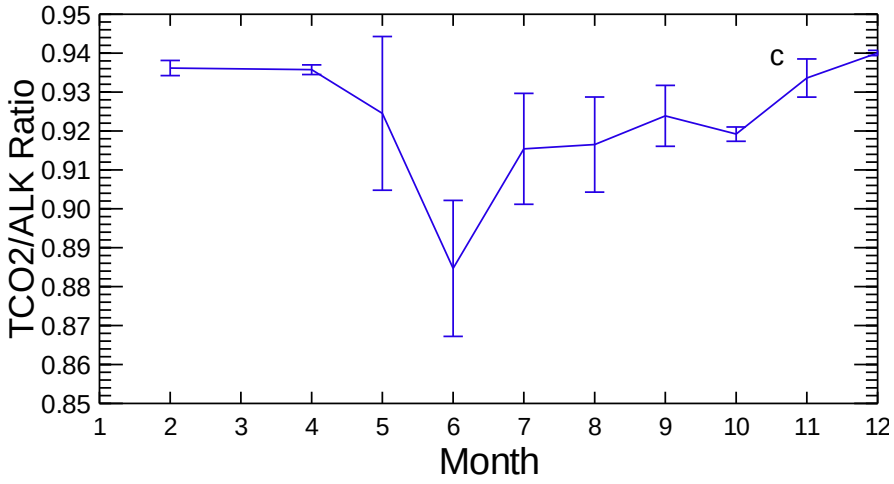


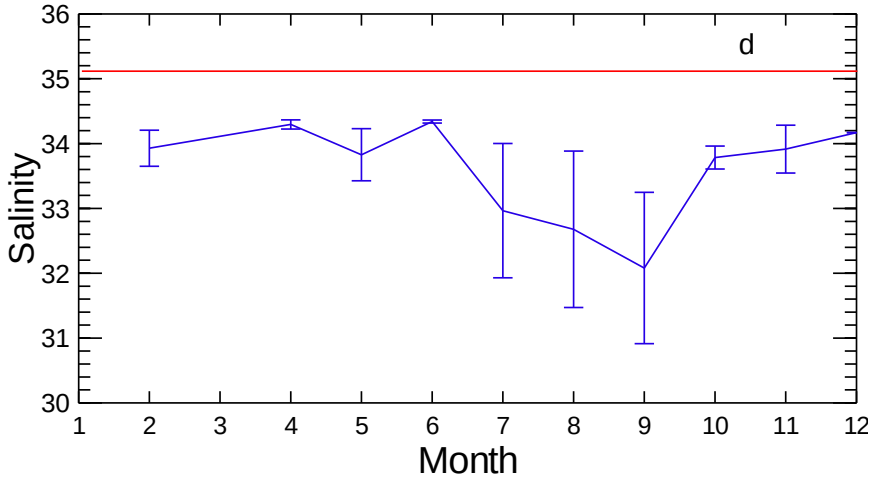


**Figure 6. Polar Water seasonal carbonate chemistry variations.** Composite Polar Water data from the 25m surface layer. The seasonal variations in the a) Total inorganic carbon/Salinity ratio, µmol $kg^{-1}$ $psu^{-1}$, b) Alkalinity/Salinity ratio, µmol $kg^{-1}$ $psu^{-1}$, and c) Total inorganic carbon/Alkalinity ratio reflect biological carbon assimilation and inorganic processes associated with fresh water inputs which lower the salinity d) to the annual

minimum in late summer. The red horizontal lines mark the Atlantic Water benchmarks (Table 2).

We take the Atlantic Water in winter (Table 2) as a proxy (benchmark) for the relatively warm and saline water advected from the North Atlantic to the Nordic Seas and the Arctic and compare with it the carbonate chemistry seasonal variations in the southward flowing Polar Water (Fig. 6). The ALK/S ratio for the Polar Water is higher than that for the Atlantic Water in winter and throughout the year (Fig. 6b). The TCO2/S ratio of the Polar Water is larger than that of the Atlantic Water except in early summer when biological assimilation, photosynthesis, decreases the TCO2 concentration. The TCO2/ALK ratio falls as a consequence (Fig. 6c) which leads to strong $pCO_2$ undersaturation and large Delta $pCO_2$ (Figs 6c and 5a). The high TCO2/S and ALK/S ratios indicate alkalinity and carbonate inputs as freshwater lowers the Polar Water salinity to a minimum in late summer (Fig. 6d).

## 4 Discussion

The Polar Water TCO2/S and ALK/S ratios (Table 2 and Fig. 6) indicate both alkalinity and dissolved carbonate additions. The choice of winter ratios (Table 2) as benchmarks is solely for the evaluation of seasonal changes in the Polar Water. Representative annual long term TCO2/S and ALK/S means would be more realistic but are not available. Still, such a TCO2/S ratio would expectedly be lower than the winter one. An assessment of the effects of the relative TCO2 and ALK additions to Polar Water depends on the benchmarks chosen (Table 2) .

The carbonate chemistry of Polar Water differs from that of open ocean waters, e.g. Atlantic Water, in having an increasingly higher alkalinity/salinity ratio+ as the salinity decreases from about S=34.4. The excess alkalinity has been attributed to the high riverine input from continents to the Arctic (Anderson et al., 2004). The flow-weighted average alkalinity of 6 major Arctic rivers, discharging 2.245 x $10^3$ $km^3$ $yr^{-1}$, is 1048 µmol $kg^{-1}$, however, without assessed uncertainty (Cooper et al., 2008). The river runoff into the Arctic is estimated to be about 4.2 x $10^3$ $km^3$ $yr^{-1}$, or 0.133 x $10^6$ $m^3$ $s^{-1}$ (0.133 Sv). This is about 11% of the global freshwater input to the oceans (Carmack et al., 2016). Taking the average alkalinity 1048 µmol $kg^{-1}$, the amount of alkalinity added by rivers to the Arctic and transported to the North Atlantic via the Canadian Arctic Archipelago and via the Fram Strait and further south with theLabrador and East Greenland Currents, would be 4.4 x $10^{12}$ mol $yr^{-1}$ (Supplement). Cooper et al. (2008) reported on riverine alkalinity but not on associated inorganic carbonate. A

418 recent assessment of Polar Water boron concentrations indicates insignificant borate
419 contribution with Arctic rivers (Olafsson et al., 2020). The riverine alkalinity may primarity
420 be attributed to carbonate alkalinity, CA=[$HCO_3^-$]+2[$CO_3^{2-}$]. The potential of the added
421 alkalinity to reduce $pCO_2$ of seawater would depend on its excess over TCO2.
422 Linear alkalinity-salinity relationships observed in the Arctic Ocean and the Nordic Seas and
423 their extrapolated intercepts to S=0, have indicated freshwater sources with alkalinity 1412
424 µmol $kg^{-1}$ (Anderson et al., 2004) and 1752 µmol $kg^{-1}$ (Nondal et al., 2009). Climatological
425 data from the West- Greenland, Iceland and Norwegian Seas show a high S=0 intercept of
426 1796 µmol $kg^{-1}$ but a lower one for the High Arctic north of 80°N, 1341 µmol $kg^{-1}$ (Takahashi
427 et al., 2014). The climatological relationships were for Potential Alkalinity, PA=TA + $NO_3^-$,
428 which has little influence since the nitrate concentrations are low. The intercepts may be
429 interpreted as the mean alkalinity of fresh waters added to the Arctic by rivers and melting ice
430 and snow. However, the above intercepts indicate considerable variability, they are also
431 higher than the average alkalinity of Arctic rivers, 1048 µmol $kg^{-1}$. The excess alkalinity
432 would lower the $pCO_2$ in seawater (and increase the pH), and thus give it an increased
433 capacity to take up $CO_2$ from the air. The thermodynamic driving force for seawater $CO_2$
434 uptake, ($pCO_{2sw} - pCO_{2a}$), would be enhanced.
435 How large is the potential effect of excess Arctic alkalinity on the $CO_2$ uptake by the Nordic
436 Seas and the North Atlantic? We consider an estimate. Suppose that the $pCO_2$ in seawater
437 was restored to the original value by absorbing $CO_2$ from the atmosphere. The carbonate
438 equilibrium relations in seawater give that $pCO_2$ is unchanged if $\Delta TCO_2 / \Delta Alk = 0.85$ Fig. S3
439 and Supplement. This ratio of additions is nearly constant in the temperature and salinity
440 range of the subarctic North Atlantic surface waters (t=5°C, S=35). The volume transport of
441 Polar Water, density <1027.8 kg $m^{-3}$, by the EGC has recently been estimated as 3.9 Sv (Våge
442 et al., 2013). Taking S=33.0 for the mean Polar Water salinity and using Equations 6 and 7 in
443 Nondal et al (2009), the mean Polar Water alkalinity is 2256 µmol $kg^{-1}$ which is 46 µmol $kg^{-1}$
444 more alkalinity than for Atlantic Water calculated at the same salinity (Nondal et al., 2009).
445 This much excess alkalinity would lower the $pCO_2$ of Atlantic Water by 88 µatm and
446 increase the pH by 0.10. Thus, the excess alkalinity advected to the North Atlantic by the
447 EGC is 5.7 x $10^{12}$ mol $yr^{-1}$. Using 0.85 for the $\Delta TCO_2/\Delta Alk$ additions at a constant $pCO_2$, we
448 obtain that the contribution of the excess EGC alkalinity to the uptake of $CO_2$ from the
449 atmosphere would be 4.8 x $10^{12}$ mol $CO_2$ $yr^{-1}$, or 0.058 Pg-C $yr^{-1}$. The estimate corresponds
450 to 21 % of the net $CO_2$ uptake of 0.27 Pg-C $yr^{-1}$ for the subarctic oceans north of 50 °N
451 (Takahashi et al., 2009). We did not include in the estimate any alkalinity contribution with

452 the considerable Canadian Arctic Archipelago Polar Water transport (Haine et al., 2015). The
453 effect of excess alkalinity on the North Atlantic $CO_2$ uptake flux may therefore be
454 substantially greater than our estimate. We note that the winter undersaturation levels, of -50
455 µatm and -35 µatm observed in the Polar and Arctic Waters, respectively (Fig. 5), translate to
456 excess alkalinity of 19 µmol $kg^{-1}$ and 21 µmol $kg^{-1}$ for further $CO_2$ influx downstream.
457 The difference between the average measured Arctic river alkalinity and the regression based
458 estimates of alkalinity sources suggests that other origins and processes than the rivers
459 contribute to the Polar Water alkalinity exported with currents from the Arctic to the Atlantic
460 Ocean. Photic layer primary production in the absence of calcification may lower the
461 TCO2/Alk ratio and seawater $pCO_2$ in marginal seas (Bates, 2006), while acidification is
462 increasing in other regions (Anderson et al., 2017;Qi et al., 2017) and projected to become
463 extensive at the end of the century (Terhaar et al., 2020). Furthermore, the sea-ice seasonal
464 formation and melting may affect the TCO2/Alk ratio (Grimm et al., 2016;Rysgaard et al.,
465 2007). Efforts to reconstruct alkalinity fields and alkalinity climatology for the Arctic have
466 however been difficult (Broullón et al., 2019).
467
468 The Arctic is complex and complex climate warming related changes are observed in the
469 western Arctic Ocean (Ouyang et al., 2020) and expected in marine freshwater systems of the
470 warming Arctic (Carmack et al., 2016). Not least is the ice cover and areas of multi-year ice
471 decreasing (Serreze and Meier, 2019). River water alkalinity increases with an addition of
472 cations derived from the chemical weathering of silicate and carbonate rocks (Berner and
473 Berner, 1987). Accordingly, an increase in Arctic weathering rates, in response to warmer
474 climate and increasing atmospheric $CO_2$, could increase the river water alkalinity transported
475 into the oceans. Such an increase would lower the $pCO_2$ in seawater and enhance the oceanic
476 uptake of atmospheric $CO_2$, providing a negative feedback mechanism to the climatic
477 warming resulting from increased atmospheric $CO_2$.
478
479 **5 Conclusions**
480 The North Atlantic region we describe has Atlantic Waters advected from southern temperate
481 latitudes and cold lower salinity Arctic and Polar Waters carried with the East Greenland
482 Current from the Arctic. The Atlantic Water seasonal $pCO_2$ variations are primarily driven by
483 regional thermal and biological cycles but without much net annual influx of $CO_2$. The
484 southward flowing Arctic and Polar Waters are on the contrary strong and persistent all year
485 $CO_2$ sinks. These waters are advected towards the sub-polar North Atlantic with high

inventories of anthropogenic carbon. The TCO2/S and ALK/S Polar Water ratios are higher than those for the Atlantic Water indicating carbonate and alkalinity sources. We point here to the Polar Water and Arctic Water $CO_2$ influx and excess alkalinity as an additional unrecognized source contributing to the North Atlantic $CO_2$ sink. We also see that there are gaps and conflicts in the knowledge about the Arctic alkalinity and carbonate budgets and that future trends in the North Atlantic $CO_2$ sink are connected to developments in the rapidly warming and changing Arctic.

**Acknowledgements**

The NMR Nordic Environmental Research Programme: Carbon Cycle and Convection in the Nordic Seas, supported the Marine Research Institute (MRI), Reykjavik, repeat station study in 1993-1995. The MRI work in 2006-2008 was supported by the European Union 6th Framework Program CARBOOCEAN, EU Contract: 511176. Taro Takahashi was supported to work on the manuscript with a grant from the the US National Oceanographic and Atmospheric Administration. The CCMP-2 wind product was generously provided from Remote Sensing Systems (www.remss.com/measurements/CCMP) by Dr. Joaquin Triñanes of CIMAS/AOML, Miami. We gratefully acknowledge the long term technical support from John Goddard and Tim Newberger, Lamont-Doherty Earth Observatory. We are grateful for the invaluable cooperation we have had with the crews of all vessels operated in this study and to Norwegian colleagues for providing time for station work in August 1994.

*Author Contributions.* J.O., T.T. and S.R.O. wrote the manuscript. J.O., Th.S.A., S.R.O. and M.D. conducted the fieldwork. J.O., T.T. S.R.O. and Th.S.A., conceived this study.

*Competing interests.* The authors declare no competing financial interests.

*Data availability.*

The underway $pCO_2$ data is available at Ocean Carbon Data System (OCADS) (Takahashi et al., 2019). The Irminger Sea and Iceland Sea seasonal study data and the Polar Water collection data are stored at the Marine and Freshwater Research Institute, Reykjavik and available by request. Irminger Sea and Iceland Sea time series data for calculation of Delta $pCO_2$ in winter is at NOAA National Centers for Environmental Information (Ólafsson, 2016, 2012).

## References


Anderson, L. G., Jutterström, S., Kaltin, S., and Jones, E. P.: Variability in river runoff distribution in the Eurasian Basin of the Arctic Ocean, Journal of Geophysical Research, 109, doi:10.1029/2003JC001733, 2004.

Anderson, L. G., Ek, J., Ericson, Y., Humborg, C., Semiletov, I., Sundbom, M., and Ulfsbo, A.: Export of calcium carbonate corrosive waters from the East Siberian Sea, Biogeosciences, 14, 1811-1823, 10.5194/bg-14-1811-2017, 2017.

Atlas, R., Hoffman, R. N., Ardizzone, J., Leidner, S. M., Jusem, J. C., Smith, D. K., and Gombos, D.: A cross-calibrated multiplatform ocean surface wind velocity product for meteorological and oceanographic applications, Bull. Amer. Meteor. Soc., 92, 157-174, 10.1109/IGARSS.2008.4778804, 2011.

Bakker, D. C. E., Pfeil, B., Landa, C. S., Metzl, N., O'Brien, K. M., Olsen, A., Smith, K., Cosca, C., Harasawa, S., Jones, S. D., Nakaoka, S., Nojiri, Y., Schuster, U., Steinhoff, T., Sweeney, C., Takahashi, T., Tilbrook, B., Wada, C., Wanninkhof, R., Alin, S. R., Balestrini, C. F., Barbero, L., Bates, N. R., Bianchi, A. A., Bonou, F., Boutin, J., Bozec, Y., Burger, E. F., Cai, W. J., Castle, R. D., Chen, L., Chierici, M., Currie, K., Evans, W., Featherstone, C., Feely, R. A., Fransson, A., Goyet, C., Greenwood, N., Gregor, L., Hankin, S., Hardman-Mountford, N. J., Harlay, J., Hauck, J., Hoppema, M., Humphreys, M. P., Hunt, C. W., Huss, B., Ibánhez, J. S. P., Johannessen, T., Keeling, R., Kitidis, V., Körtzinger, A., Kozyr, A., Krasakopoulou, E., Kuwata, A., Landschützer, P., Lauvset, S. K., Lefèvre, N., Lo Monaco, C., Manke, A., Mathis, J. T., Merlivat, L., Millero, F. J., Monteiro, P. M. S., Munro, D. R., Murata, A., Newberger, T., Omar, A. M., Ono, T., Paterson, K., Pearce, D., Pierrot, D., Robbins, L. L., Saito, S., Salisbury, J., Schlitzer, R., Schneider, B., Schweitzer, R., Sieger, R., Skjelvan, I., Sullivan, K. F., Sutherland, S. C., Sutton, A. J., Tadokoro, K., Telszewski, M., Tuma, M., van Heuven, S. M. A. C., Vandemark, D., Ward, B., Watson, A. J., and Xu, S.: A multi-decade record of high-quality fCO2 data in version 3 of the Surface Ocean CO2 Atlas (SOCAT), Earth Syst. Sci. Data, 8, 383-413, 10.5194/essd-8-383-2016, 2016.

Bates, N. R., Takahashi, T., Chipman, D. W., and Knap, A. H.: Variability of $pCO_2$ on diel to seasonal timescales in the Sargasso Sea near Bermuda, Journal of Geophysical Research: Oceans, 103, 15567-15585, 10.1029/98jc00247, 1998.

Bates, N. R.: Air-sea $CO_2$ fluxes and the continental shelf pump of carbon in the Chukchi Sea adjacent to the Arctic Ocean, Journal of Geophysical Research: Oceans, 111, 10.1029/2005jc003083, 2006.

Berner, E. K., and Berner, R. A.: The Global Water Cycle, Geochemistry and Environment, Prentice-Hall, Englewood Cliffs, NJ, 1987.

Broecker, W. S.: The Great Ocean Conveyor, Oceanography, 4, 79-89, 1991.

Broullón, D., Pérez, F. F., Velo, A., Hoppema, M., Olsen, A., Takahashi, T., Key, R. M., Tanhua, T., González-Dávila, M., Jeansson, E., Kozyr, A., and van Heuven, S. M. A. C.: A global monthly climatology of total alkalinity: a neural network approach, Earth Syst. Sci. Data, 11, 1109-1127, 10.5194/essd-11-1109-2019, 2019.

Carmack, E. C., Yamamoto-Kawai, M., Haine, T. W. N., Bacon, S., Bluhm, B. A., Lique, C., Melling, H., Polyakov, I. V., Straneo, F., Timmermans, M.-L., and Williams, W. J.: Freshwater and its role in the Arctic Marine System: Sources, disposition, storage, export, and physical and biogeochemical consequences in the Arctic and global oceans, J. Geophys. Res. Biogeosci., 121, 675–717, doi:10.1002/2015JG003140, 2016.

Chipman, D., Marra, J., and Takahashi, T.: Primary production at 47°N and 20°W in the North Atlantic Ocean: a comparision between the $^{14}C$ incubation method and the mixed layer budget, Deep Sea Research II, 40, 151-169, 1993.

570 Cooper, L. W., McClelland, J. W., Holmes, R. M., Raymond, P. A., Gibson, J. J., C. K. Guay,
571 and Peterson, B. J.: Flow-weighted values of runoff tracers ($\delta^{18}O$, DOC, Ba, alkalinity) from
572 the six largest Arctic rivers, Geophysical Research Letters, 35, doi:10.1029/2008GL035007,
573 2008.
574 Dickson, A. G.: Standard Potential of the Reaction - AgCl(S)+1/2$H_2$(G)=Ag(S)+HC l(Aq)
575 and the Standard Acidity Constant of the ion $HSO_4^-$ in Synthetic Sea-Water from 273.15-K to
576 318.15-K, J Chem Thermodyn, 22, 113-127, Doi 10.1016/0021-9614(90)90074-Z, 1990.
577 Dickson, R. P., Meincke, J., Malmberg, S. A., and Lee, A. J.: The Great salinity Anomaly in
578 the northern North Atlantic, Progress in Oceanography, 20, 103-151, 1988.
579 Fay, A. R., and McKinley, G. A.: Global open-ocean biomes: mean and temporal variability,
580 Earth Syst. Sci. Data, 6, 273-284, 10.5194/essd-6-273-2014, 2014.
581 Flatau, M. K., Talley, L., and Niiler, P. P.: The North Atlantic Oscillation, surface current
582 velocities, and SST changes in the subpolar North Atlantic, Journal of Climate, 16, 2355-
583 2369, 2003.
584 Friedlingstein, P., Jones, M. W., O'Sullivan, M., Andrew, R. M., Hauck, J., Peters, G. P.,
585 Peters, W., Pongratz, J., Sitch, S., Le Quéré, C., Bakker, D. C. E., Canadell, J. G., Ciais, P.,
586 Jackson, R. B., Anthoni, P., Barbero, L., Bastos, A., Bastrikov, V., Becker, M., Bopp, L.,
587 Buitenhuis, E., Chandra, N., Chevallier, F., Chini, L. P., Currie, K. I., Feely, R. A., Gehlen,
588 M., Gilfillan, D., Gkritzalis, T., Goll, D. S., Gruber, N., Gutekunst, S., Harris, I., Haverd, V.,
589 Houghton, R. A., Hurtt, G., Ilyina, T., Jain, A. K., Joetzjer, E., Kaplan, J. O., Kato, E., Klein
590 Goldewijk, K., Korsbakken, J. I., Landschützer, P., Lauvset, S. K., Lefèvre, N., Lenton, A.,
591 Lienert, S., Lombardozzi, D., Marland, G., McGuire, P. C., Melton, J. R., Metzl, N., Munro,
592 D. R., Nabel, J. E. M. S., Nakaoka, S. I., Neill, C., Omar, A. M., Ono, T., Peregon, A., Pierrot,
593 D., Poulter, B., Rehder, G., Resplandy, L., Robertson, E., Rödenbeck, C., Séférian, R.,
594 Schwinger, J., Smith, N., Tans, P. P., Tian, H., Tilbrook, B., Tubiello, F. N., van der Werf, G.
595 R., Wiltshire, A. J., and Zaehle, S.: Global Carbon Budget 2019, Earth Syst. Sci. Data, 11,
596 1783-1838, 10.5194/essd-11-1783-2019, 2019.
597 GLOBALVIEW-CO2: Cooperative Global Atmospheric Data Integration Project. 2013,
598 updated annually. Multi-laboratory compilation of synchronized and gap-filled atmospheric
599 carbon dioxide records for the period 1979-2012 obspack_co2_1_GLOBALVIEW-
600 CO2_2013_v1.0.4_2013-12-23, 2013.
601 Grimm, R., Notz, D., Glud, R. N., Rysgaard, S., and Six, K. D.: Assessment of the sea-ice
602 carbon pump: Insights from a three-dimensional ocean-sea-ice-biogeochemical model
603 (MPIOM/HAMOCC), Elementa: Science of the Anthropocene, 4, doi:
604 10.12952/journal.elementa.000136
605 elementascience.org, 2016.
606 Gruber, N., Clement, D., Carter, B. R., Feely, R. A., van Heuven, S., Hoppema, M., Ishii, M.,
607 Key, R. M., Kozyr, A., Lauvset, S. K., Lo Monaco, C., Mathis, J. T., Murata, A., Olsen, A.,
608 Perez, F. F., Sabine, C. L., Tanhua, T., and Wanninkhof, R.: The oceanic sink for
609 anthropogenic $CO_2$ from 1994 to 2007, Science, 363, 1193-1199, 10.1126/science.aau5153,
610 2019.
611 Haine, T. W. N., Curry, B., Gerdes, R., Hansen, E., Karcher, M., Lee, C., Rudels, B., Spreen,
612 G., Steur, L. d., Stewart, K. D., and Woodgate, R.: Arctic freshwater export: Status,
613 mechanisms, and prospects, Global and Planetary Change, 125, 13-35, 2015.
614 Håvik, L., Pickart, R. S., Våge, K., Torres, D., Thurnherr, A. M., Beszczynska-Möller, A.,
615 Walczowski, W., and Appen, W.-J. v.: Evolution of the East Greenland Current from Fram
616 Strait to Denmark Strait: Synoptic measurements from summer 2012, J. Geophys. Res.
617 Oceans, 122, 1974-1994, doi:10.1002/2016JC01222, 2017.
618 Hátún, H., Sandø, A. B., Drange, H., Hansen, B., and Valdimarsson, H.: Influence of the
619 Atlantic Subpolar Gyre on the Thermohaline Circulation, Science, 309, 1841-1844, 2005.

Holliday, N. P., Bersch, M., Berx, B., Chafik, L., Cunningham, S., Florindo-López, C., Hátún, H., Johns, W., Josey, S. A., Larsen, K. M. H., Mulet, S., Oltmanns, M., Reverdin, G., Rossby, T., Thierry, V., Valdimarsson, H., and Yashayaev, I.: Ocean circulation causes the largest freshening event for 120 years in eastern subpolar North Atlantic, Nature Communications, 11, 585, 10.1038/s41467-020-14474-y, 2020.

Khatiwala, S., Tanhua, T., Mikaloff Fletcher, S., Gerber, M., Doney, S. C., Graven, H. D., Gruber, N., McKinley, G. A., Murata, A., Ríos, A. F., and Sabine, C. L.: Global ocean storage of anthropogenic carbon, Biogeosciences, 10, 2169-2191, 10.5194/bg-10-2169-2013, 2013.

Landschützer, P., Gruber, N., Bakker, D. C. E., Schuster, U., Nakaoka, S., Payne, M. R., Sasse, T. P., and Zeng, J.: A neural network-based estimate of the seasonal to inter-annual variability of the Atlantic Ocean carbon sink, Biogeosciences, 10, 7793-7815, 10.5194/bg-10-7793-2013, 2013.

Lebehot, A. D., Halloran, P. R., Watson, A. J., McNeall, D., Ford, D. A., Landschützer, P., Lauvset, S. K., and Schuster, U.: Reconciling Observation and Model Trends in North Atlantic Surface $CO_2$, Global Biogeochemical Cycles, 33, 1204–1222, 10.1029/2019gb006186, 2019.

Lee, K., Kim, T.-W., Byrne, R. H., Millero, F. J., Feely, R. A., and Liu, Y.-M.: The universal ratio of boron to chlorinity for the North Pacific and North Atlantic oceans, Geochimica et Cosmochimica Acta, 74, 1801–1811, 2010.

Lewis, E., and Wallace, D.: Programme developed for $CO_2$ system calculations, Carbon Dioxide Information Analysis Center, Oak Ridge National Laboratory, U.S. Department of EnergyORNL/CDIAC-105, 1998.

Lueker, T. J., Dickson, A. G., and Keeling, C. D.: Ocean $pCO_2$ calculated from dissolved inorganic carbon, alkalinity, and equations for K-1 and K-2: validation based on laboratory measurements of $CO_2$ in gas and seawater at equilibrium, Marine Chemistry, 70, 105-119, Doi 10.1016/S0304-4203(00)00022-0, 2000.

McClelland, J. W., Holmes, R. M., Dunton, K. H., and Macdonald, R. W.: The Arctic Ocean Estuary, Estuaries and Coasts, 35, 353–368, DOI 10.1007/s12237-010-9357-3, 2012.

McKinley, G. A., Fay, A. R., Lovenduski, N. S., and Pilcher, D. J.: Natural Variability and Anthropogenic Trends in the Ocean Carbon Sink, Annu. Rev. Mar. Sci., 9, 125-150, 10.1146/annurev-marine-010816-060529, 2017.

Mikaloff Fletcher, S. E., Gruber, N., Jacobson, A. R., Doney, S. C., Dutkiewicz, S., Gerber, M., Follows, M., Joos, F., Lindsay, K., Menemenlis, D., Mouchet, A., ller, S. A. M., Sarmiento, J. L., et al. (2006), and Global Biogeochem. Cycles, GB2002, doi:10.1029/2005GB002530.: Inverse estimates of anthropogenic $CO_2$ uptake, transport, and storage by the ocean, Global Biogeochem. Cycles, 20, doi:10.1029/2005GB002530, 2006.

Nilsen, J. E. Ø., Hátún, H., Mork, K. A., and Valdimarsson, H.: The NISE Dataset. , Faroese Fisheries Laboratory, Box 3051, Tórshavn, Faroe Islands, 2008.

Nondal, G., Bellerby, R., Olsen, A., Johannessen, T., and Olafsson, J.: Predicting the surface ocean $CO_2$ system in the northern North Atlantic: Implications for the use of Voluntary Observing Ships., Limnology and Oceanography: Methods, 7, 109-118, 2009.

Olafsson, J., Olafsdottir, S. R., Benoit-Cattin, A., Danielsen, M., Arnarson, T. S., and Takahashi, T.: Rate of Iceland Sea acidification from time series measurements, Biogeosciences, 6, 2661-2668, 2009.

Olafsson, J., Olafsdottir, S. R., Benoit-Cattin, A., and Takahashi, T.: The Irminger Sea and the Iceland Sea time series measurements of sea water carbon and nutrient chemistry 1983–2008, Earth Syst. Sci. Data, 2, 99-104, 10.5194/essd-2-99-2010, 2010.

Olafsson, J., Lee, K., Olafsdottir, S. R., Benoit-Cattin, A., Lee, C.-H., and Kim, M.: Boron to salinity ratios for Atlantic, Arctic and Polar Waters: A view from downstream, Marine Chemistry, 224, 103809, https://doi.org/10.1016/j.marchem.2020.103809, 2020.

Olsen, A., Omar, A. M., Bellerby, R. G. J., Johannessen, T., Ninnemann, U., Brown, K. R., Olsson, K. A., Olafsson, J., Nondal, G., Kivimae, C., Kringstad, S., Neill, C., and Olafsdottir, S.: Magnitude and Origin of the Anthropogenic $CO_2$ Increase and $^{13}C$ Suess Effect in the Nordic Seas Since 1981, Global Biogeochemical Cycles, 20, GB3027, doi:10.1029/2005GB002669, 2006.
Ouyang, Z., Qi, D., Chen, L., Takahashi, T., Zhong, W., DeGrandpre, M. D., Chen, B., Gao, Z., Nishino, S., Murata, A., Sun, H., Robbins, L. L., Jin, M., and Cai, W.-J.: Sea-ice loss amplifies summertime decadal CO2 increase in the western Arctic Ocean, Nature Climate Change, 10, 678-684, 10.1038/s41558-020-0784-2, 2020.
Ólafsson, J.: Connections between oceanic conditions off N-Iceland, Lake Mývatn temperature, regional wind direction variability and the North Atlantic Oscillation, Rit Fiskideildar, 16, 41-57, 1999.
Ólafsson, J.: Winter mixed layer nutrients in the Irminger and Iceland Seas, 1990-2000, ICES Marine Science Symposia, 219, 329-332, 2003.
Ólafsson, J.: Partial pressure (or fugacity) of carbon dioxide, dissolved inorganic carbon, temperature, salinity and other variables collected from discrete samples, profile and time series profile observations during the R/Vs Arni Fridriksson and Bjarni Saemundsson time series IcelandSea (LN6) cruises in the North Atlantic Ocean from 1985-02-22 to 2013-11-26 (NCEI Accession 0100063). Information, N. N. C. f. E. (Ed.), NOAA National Centers for Environmental Information, 2012.
Ólafsson, J.: Partial pressure (or fugacity) of carbon dioxide, dissolved inorganic carbon, temperature, salinity and other variables collected from discrete sample and profile observations using CTD, bottle and other instruments from ARNI FRIDRIKSSON and BJARNI SAEMUNDSSON in the North Atlantic Ocean from 1983-03-05 to 2013-11-13 (NCEI Accession 0149098). Information, N. N. C. f. E. (Ed.), 2016.
Peng, T.-H., Takahashi, T., Broecker, W. S., and Ólafsson, J.: Seasonal variability of carbon dioxide, nutrients and oxygen in the northern North Atlantic surface water, Tellus, 39B, 439-458, 1987.
Pierrot, D., Lewis, E., and Wallace, D. W. R.: MS Excel Program Developed for CO2 System Calculations. ORNL/CDIAC-105a. Carbon Dioxide Information Analysis Center, doi: 10.3334/CDIAC/otg.CO2SYS_XLS_CDIAC105a. Oak Ridge National Laboratory, U.S. Department of Energy, Oak Ridge, Tennessee., Oak Ridge, Tennessee, 2006.
Qi, D., Chen, L., Chen, B., Gao, Z., Zhong, W., Feely, R. A., Anderson, L. G., Sun, H., Chen, J., Chen, M., Zhan, L., Zhang, Y., and Cai, W.-J.: Increase in acidifying water in the western Arctic Ocean, Nature Clim. Change, 7, 195-199, 10.1038/nclimate3228 http://www.nature.com/nclimate/journal/v7/n3/abs/nclimate3228.html#supplementary-information, 2017.
Reverdin, G., Metzl, N., Olafsdottir, S., Racapé, V., Takahashi, T., Benetti, M., Valdimarsson, H., Benoit-Cattin, A., Danielsen, M., Fin, J., Naamar, A., Pierrot, D., Sullivan, K., Bringas, F., and Goni, G.: SURATLANT: a 1993–2017 surface sampling in the central part of the North Atlantic subpolar gyre, Earth Syst. Sci. Data, 10, 1901-1924, 10.5194/essd-10-1901-2018, 2018.
Rysgaard, S., Glud, R. N., Sejr, M. K., Bendtsen, J., and Christensen, P. B.: Inorganic carbon transport during sea ice growth and decay: A carbon pump in polar seas, Journal of Geophysical Research, 112, 2007.
Schlitzer, R.: Ocean Data View, http://odv.awi.de, 2018.
Schuster, U., McKinley, G. A., Bates, N., Chevallier, F., Doney, S. C., Fay, A. R., González-Dávila, M., Gruber, N., Jones, S., Krijnen, J., Landschützer, P., Lefèvre, N., Manizza, M., Mathis, J., Metzl, N., Olsen, A., Rios, A. F., Rödenbeck, C., Santana-Casiano, J. M., Takahashi, T., Wanninkhof, R., and Watson, A. J.: An assessment of the Atlantic and Arctic

sea–air $CO_2$ fluxes, 1990–2009, Biogeosciences, 10, 607-627, 10.5194/bg-10-607-2013, 2013.
Serreze, M. C., and Meier, W. N.: The Arctic's sea ice cover: trends, variability, predictability, and comparisons to the Antarctic, Annals of the New York Academy of Sciences, 1436, 36-53, 10.1111/nyas.13856, 2019.
Stefánsson, U.: North Icelandic Waters, Rit Fiskideildar, 3, 1-269, 1962.
Sutherland, D. A., Pickart, R. S., Peter Jones, E., Azetsu-Scott, K., Jane Eert, A., and Ólafsson, J.: Freshwater composition of the waters off southeast Greenland and their link to the Arctic Ocean, Journal of Geophysical Research: Oceans, 114, 10.1029/2008jc004808, 2009.
Takahashi, T., Ólafsson, J., Broecker, W. S., Goddard, J., Chipman, D. W., and White, J.: Seasonal variability of the carbon-nutrient chemistry in the ocean areas west and north of Iceland, Rit Fiskideildar, 9, 20-36, 1985.
Takahashi, T., Ólafsson, J., Goddard, J. G., Chipman, D. W., and Sutherland, S. C.: Seasonal variation of $CO_2$ and nutrient salts over the high latitude oceans: A comparative study, Global Biogeochemical Cycles, 7, 843-878, 1993.
Takahashi, T., Sutherland, S. C., Sweeney, C., Poisson, A., Metzl, N., Tilbrook, T., Bates, N., Wanninkhof, R., Feely, R. A., Sabine, C., Olafsson, J., and Nojiri, Y.: Global sea-air $CO_2$ flux based on climatological suface ocean $pCO_2$, and seasonal biological and temperature effects, Deep-Sea Research II, 49, 1601-1622, 2002.
Takahashi, T., Sutherland, S. C., Wanninkhof, R., Sweeney, C., Feely, R. A., Chipman, D. W., Hales, B., Friederich, G., Chavez, F., Sabine, C., Watson, A., Bakker, D. C. E., Schuster, U., Metzl, N., Yoshikawa-Inoue, H., Ishii, M., Midorikawa, T., Nojiri, Y., Körtzinger, A., Steinhoff, T., Hoppema, M., Olafsson, J., Arnarson, T. S., Tilbrook, B., Johannessen, T., Olsen, A., Bellerby, R., Wong, C. S., Delille, B., Bates, N. R., and Baar, H. J. W. d.: Climatological mean and decadal change in surface ocean $pCO_2$, and net sea-air $CO_2$ flux over the global oceans, Deep-Sea Research II, 56, 554-577, doi:10.1016/j.dsr2.2008.12.009, 2009.
Takahashi, T., Sutherland, S. C., Chipman, D. W., Goddard, J. G., Ho, C., Newberger, T., Sweeney, C., and Munro, D. R.: Climatological distributions of pH, $pCO_2$, total $CO_2$, alkalinity, and $CaCO_3$ saturation in the global surface ocean, and temporal changes at selected locations, Marine Chemistry, 164, 95-125, http://dx.doi.org/10.1016/j.marchem.2014.06.004, 2014.
Takahashi, T., Sutherland, S. C., and Kozyr, A.: Global Ocean Surface Water Partial Pressure of $CO_2$ Database: Measurements Performed During 1957-2018 (LDEO Database Version 2018) (NCEI Accession 0160492). Version 7.7. NOAA National Centers for Environmental Information. National Centers for Environmental Information, 2019.
Tans, P., and Keeling, R.: Mauna Loa $CO_2$ monthly mean data. NOAA/ESRL (Ed.), 2019.
Terhaar, J., Kwiatkowski, L., and Bopp, L.: Emergent constraint on Arctic Ocean acidification in the twenty-first century, Nature, 582, 379-383, 10.1038/s41586-020-2360-3, 2020.
Våge, K., Pickart, R. S., Sarafanov, A., Knutsen, Ø., Mercier, H., Lherminier, P., van Aken, H. M., Meincke, J., Quadfasel, D., and Bacon, S.: The Irminger Gyre: Circulation, convection, and interannual variability, Deep Sea Research Part I: Oceanographic Research Papers, 58, 590-614, https://doi.org/10.1016/j.dsr.2011.03.001, 2011.
Våge, K., Pickart, R. S., Spall, M. A., Moore, G. W. K., Valdimarsson, H., Torres, D. J., Y.Erofeeva, S., and Ø.Nilsen, J. E.: Revised circulation scheme north of the Denmark Strait, Deep-Sea Research Part I, 79, 20–39, 2013.

Våge, K., Moore, G. W. K., Jónsson, S., and Valdimarsson, H.: Water mass transformation in the Iceland Sea, Deep Sea Research Part I: Oceanographic Research Papers, 101, 98-109, http://dx.doi.org/10.1016/j.dsr.2015.04.001, 2015.
Wanninkhof, R., Park, G. H., Takahashi, T., Sweeney, C., Feely, R., Nojiri, Y., Gruber, N., Doney, S. C., McKinley, G. A., Lenton, A., Le Quéré, C., Heinze, C., Schwinger, J., Graven, H., and Khatiwala, S.: Global ocean carbon uptake: magnitude, variability and trends, Biogeosciences, 10, 1983-2000, 10.5194/bg-10-1983-2013, 2013.
Wanninkhof, R.: Relationship between wind speed and gas exchange over the ocean revisited, Limnol. Oceanogr.: Methods, 12, 351–362, DOI 10.4319/lom.2014.12.351, 2014.
Wanninkhof, R., and Triñanes, J.: The impact of changing wind speeds on gas transfer and its effect on global air-sea $CO_2$ fluxes, Global Biogeochem. Cycles, 31, doi:10.1002/2016GB005592, 2017.
Watson, A. J., Schuster, U., Shutler, J. D., Holding, T., Ashton, I. G. C., Landschützer, P., Woolf, D. K., and Goddijn-Murphy, L.: Revised estimates of ocean-atmosphere CO2 flux are consistent with ocean carbon inventory, Nature Communications, 11, 4422, 10.1038/s41467-020-18203-3, 2020.
Weiss, R. F.: Carbon dioxide in water and seawater: The solubility of a non-ideal gas, Marine Chemistry, 2, 203-215, 1974.
Weiss, R. F., and Price, B. A.: Nitrous oxide solubility in water and seawater, Marine Chemistry, 8, 347-359, https://doi.org/10.1016/0304-4203(80)90024-9, 1980.